Title no. 108-M56

Diverse Embedment Model for Steel Fiber-Reinforced Concrete in Tension: Model Verification

by Seong-Cheol Lee, Jae-Yeol Cho, and Frank J. Vecchio

In this paper, results obtained from the Diverse Embedment Model (DEM) for analysis of steel fiber-reinforced concrete, described in an accompanying paper, are compared with experimental results produced by several independent researchers. Variation of the fiber orientation factor, which accounts for the effects of finite member dimensions on fiber orientation and embedment, is also theoretically investigated and compared with experimental data. Verification studies show that the proposed model provides accurate predictions of the tensile stress and crack width relationship of uniaxial tension specimens containing straight or end-hooked steel fibers. In addition, the proposed model provides accurate calculations of the distribution of tensile stress provided by fibers. The proposed model is also shown to be useful in modeling aspects of the tensile behavior, such as crack spacing and tension stiffening, of fiber-reinforced concrete (FRC) members reinforced with ordinary steel reinforcing bars.

Keywords: anchorage; bond; end-hooked fiber; fiber orientation factor; member size; steel fiber-reinforced concrete; straight fiber; tensile stress.

INTRODUCTION

Fiber-reinforced concrete (FRC) elements subjected to tension typically exhibit a ductile response because the fibers bridging across the cracks compensate for the brittle and nonductile behavior of the concrete matrix. Over the last several decades, to better model the tensile behavior of FRC, numerous theoretical investigations have been conducted. These studies can be classified into two groups: analytical models,[1-4] considering the pullout behavior of single steel fiber; and analytical models,[5-8] considering the random distribution of fibers in FRC.

Combining the two types of models has been problematic. The analysis models,[1-4] developed only for the pullout behavior of a single steel fiber, cannot be applied to the prediction of the tensile behavior of FRC members in which fibers are randomly distributed and where the bond characteristics between fiber and concrete matrix as well as the mechanical anchorage effect of end-hooked steel fiber are considered; the resulting calculations are too complex. On the other hand, the analytical models,[5-8] considering the random distribution of fibers, typically assumed uniform bond stress along the fiber length for both straight and end-hooked fibers. Moreover, finite member dimensions, which may have considerable effect on the random distribution of fibers, are generally not considered in previous models,[5-7] even though the sizes of the specimens used for verification of the analytical models are commonly relatively small compared with fiber length. To overcome these deficiencies, the Diverse Embedment Model (DEM) was derived for steel fiber-reinforced concrete (SFRC) members subjected to uniaxial tension; formulation of the model was presented in an accompanying paper.[9] The proposed analysis model considers not only the effect of member dimension but also the pullout characteristics of steel fibers inclusive of the frictional bond behavior of straight fibers as well as the mechanical anchorage effect of end-hooked steel fibers.

In this paper, verification of the DEM is undertaken by comparing the predictions of the model against experimental results reported by several independent researchers.[10-13] The effect of the pullout characteristics of steel fibers and the effect of member dimension on the tensile behavior of SFRC members are also discussed.

RESEARCH SIGNIFICANCE

A rational comprehensive model for the tensile behavior of SFRC should consider various factors and mechanisms, including the pullout behavior of individual fibers, the random distribution of fibers, and the effects of finite member dimensions. While such a model has been elusive in the past, the proposed DEM represents a significant effort toward achieving this goal. Verification studies will show that the proposed model provides good agreement with experimental results, including accurate predictions of tensile stress and crack width relationships and variations in the fiber orientation factor. Moreover, the proposed model enables calculation of the distribution of tensile stresses provided by fibers and concrete matrix between cracks. Thus, it can be a useful tool in the modeling of the tensile behavior of SFRC members, including such members also reinforced with conventional reinforcing bar.

SUMMARY OF PROPOSED ANALYSIS MODEL

The fiber tensile stress at a crack can be calculated from the analysis for the pullout behavior of a fiber embedded on both sides. In this analysis of a single fiber, the pullout characteristics such as the frictional bond behavior of a straight fiber and the mechanical anchorage effect of an end-hooked fiber are taken into account. Because the fiber tensile stress at a crack is significantly affected by the fiber inclination angle and fiber embedment length, the average fiber tensile stress at a crack can be described for three-dimensional (3-D) infinite elements with the following equation[9]

$$\sigma_{f,cr,avg} = \frac{2}{l_f} \int_0^{l_f/2} \int_0^{\pi/2} \sigma_{f,cr}\left(l_a, \theta\right) \sin\theta \, d\theta \, dl_a \qquad (1)$$

In Eq. (1), from the accompanying paper,[9] the probability function for the fiber inclination angle, $\sin\theta$, can be appropriately modified for two- or three-dimensional

ACI member **Seong-Cheol Lee** is a Postdoctoral Researcher in the Department of Civil Engineering at the University of Toronto, Toronto, ON, Canada. He received his PhD from Seoul National University, Seoul, Korea, in 2007. His research interests include the shear behavior of concrete structures and the analysis of prestressed concrete structures and fiber-reinforced concrete members.

ACI member **Jae-Yeol Cho** is an Assistant Professor in the Department of Civil and Environmental Engineering at Seoul National University, where he also received his PhD. His research interests include nonlinear analysis and optimized design of reinforced and prestressed concrete structures, material modeling, and similitude laws for dynamic testing of concrete structures.

Frank J. Vecchio, FACI, is a Professor in the Department of Civil Engineering at the University of Toronto. He is a member of Joint ACI-ASCE Committees 441, Reinforced Concrete Columns, and 447, Finite Element Analysis of Reinforced Concrete Structures. His research interests include nonlinear analysis and design of reinforced concrete structures, constitutive modeling, performance assessment and forensic investigation, and repair and rehabilitation of structures.

elements in which the fiber orientation can be significantly affected by boundary surfaces.

From the average fiber stress at a crack, the tensile stress attained by fibers in FRC members can be calculated by considering the fiber orientation factor and the fiber volumetric ratio as follows

$$f_f = \alpha_f V_f \sigma_{f,cr,avg} \qquad (2)$$

The fiber orientation factor can also be modified with the probability function for the fiber inclination angle for non-infinite members. Details are presented in an accompanying paper.[9]

FIBER ORIENTATION FACTOR CONSIDERING MEMBER DIMENSION

In this section, the effect of member dimension on the fiber orientation factor will be discussed along with the equations derived in this research.[9] For verification of the proposed model regarding fiber orientation factor, the calculated values will be compared with the results measured by Soroushian and Lee.[12]

Effect of member dimension on fiber orientation factor

As previously derived,[9] the fiber orientation factor varies in regions where the distance to a boundary surface is less than the fiber length because the fiber inclination angle herein is affected by the surface. Figure 1 shows the variation of the fiber orientation factor considering the influence of two-dimensional (2-D) member thicknesses larger than two times the fiber length. This plot was obtained from Eq. (24b) in Reference 9. At the boundary surface, because out-of-plane fiber inclinations are assumed to not be allowed, the fiber orientation factor becomes $2/\pi$; this result is the same as that presented by Aveston and Kelly[14] and Stroeven[8] for randomly distributed fibers in a plane. In addition to this, the variation of the fiber orientation factor considering variable member dimensions in 2-D or 3-D has been derived in the accompanying paper.[9] Moving inward away from all boundaries, the factor converges to 0.5. Thus, for an infinite 2-D element, the fiber orientation factor can be assumed to be constant at 0.5 at distances from the boundary surface equal to or greater than the fiber length. The member
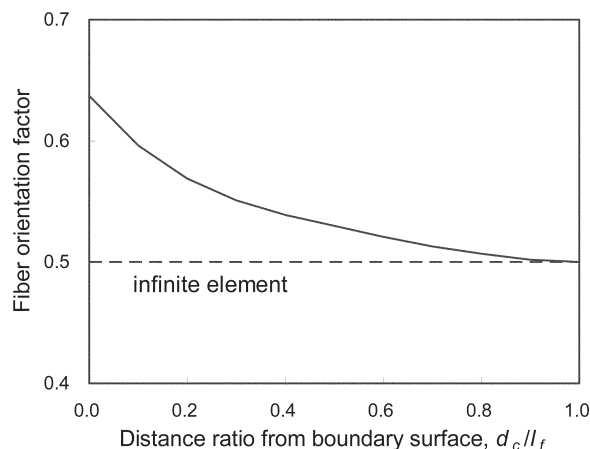

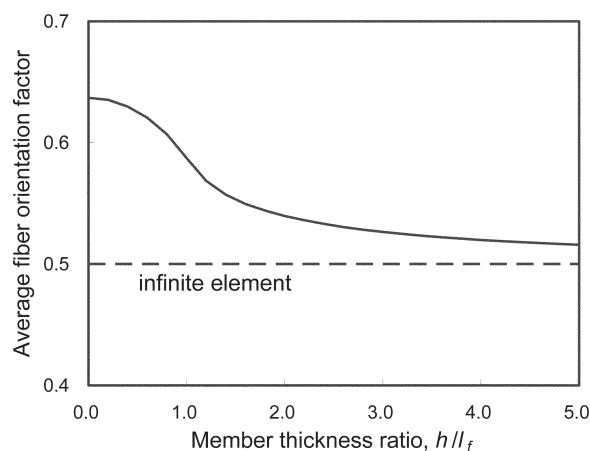Fig. 1—Variation of local fiber orientation factor in 2-D element.

Fig. 2—Average fiber orientation factor in 2-D element.

thickness effect on the fiber orientation factor, averaged over the thickness as defined by Eq. (3), is illustrated in Fig. 2.

$$\alpha_{f,avg} = \int_h \alpha_f \, dh \qquad (3)$$

As shown in Fig. 2, the average fiber orientation factor varies from $2/\pi$ to 0.5 with increasing member thickness. When the member thickness is less than two times the fiber length ($h/l_f < 2.0$), it can be seen that the effect of member thickness on the average fiber orientation factor is especially significant because the distribution of fiber inclination angle is influenced by both surfaces at once. It can be concluded, therefore, that when the member thickness is less than two times the fiber length, the effect of member thickness should be considered when evaluating the tensile stress provided by the fibers, which is directly affected by the fiber orientation factor.

In the same manner as for a 2-D element, the variation of the fiber orientation factor within the cross section of a 3-D member can be calculated (refer to Eq. (24c) in Reference 9). Figure 3 describes the variation of the fiber orientation factor in rectangular sections having the dimensions $2.0l_f \times 1.4l_f$ and $1.67l_f \times 1.0l_f$; such sized cross sections have commonly been for uniaxial tension tests by several researchers.[10,11,13] Note that the crack surface is assumed to be perpendicular to
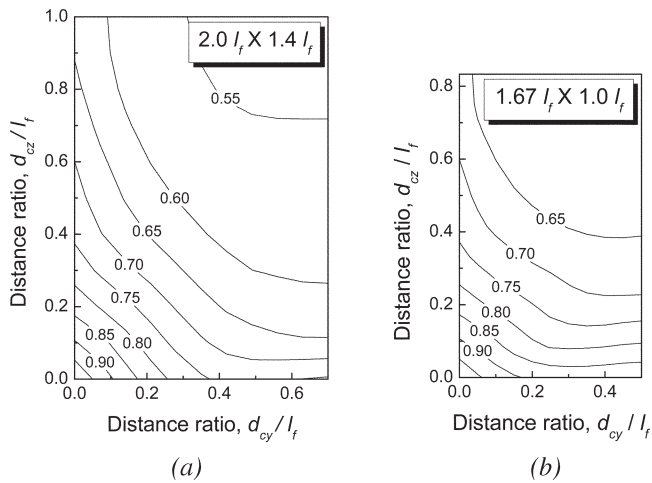
Fig. 3—Variation of local fiber orientation factor in 3-D element with rectangular section: (a) $2.0l_f \times 1.4l_f$; and (b) $1.67l_f \times 1.0l_f$.
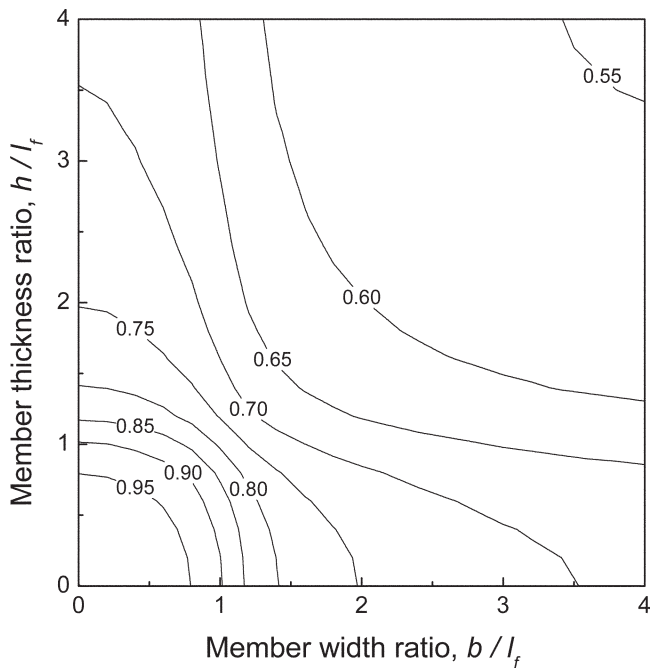

Fig. 4—Average fiber orientation factor in 3-D element with rectangular section.

Fig. 5—Fiber orientation factors measured by Soroushian and Lee.[12]

both boundary surfaces. As shown in these figures, the fiber orientation factor at the exterior corner of the section (corresponding to the origin of each graph) is 1.0, because all fibers at the corner are assumed to be aligned in the direction perpendicular to the crack surface. With increasing distance from the boundary surfaces, the fiber orientation factor decreases toward the asymptotic value of 0.5. The average fiber orientation factor is generally larger in members with smaller cross sections. For example, comparing Fig. 3(a) and 3(b), it can be deduced that the fiber orientation factor averaged over the cross section is 0.629 for the larger member ($2.0l_f \times 1.4l_f$) and 0.695 for the smaller member ($1.67l_f \times 1.0l_f$). The effect of member dimensions on the fiber orientation factor average value for a cross section is illustrated in Fig. 4. As shown by this figure, the average factor is significantly affected by the
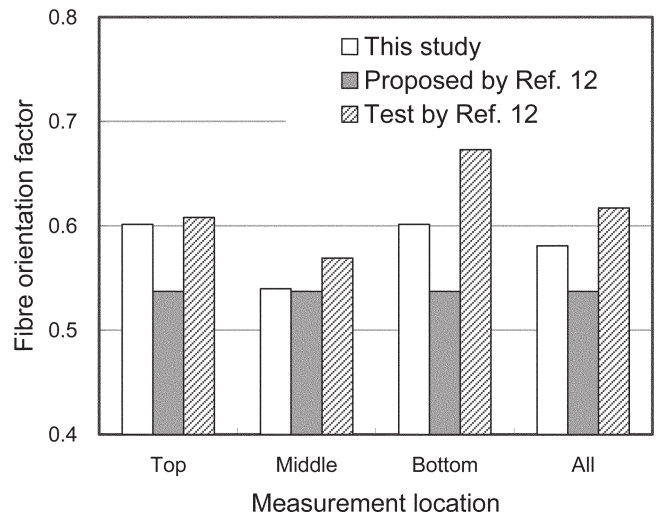
member dimensions, especially when the thickness or width is less than two times the fiber length. Consequently, this result indicates that the fiber orientation factor should be considered when a real structure, for which the dimension effect is negligible because of its large size, is modeled using FRC tensile properties taken from uniaxial tension tests performed on specimens having relatively small dimensions compared to the fiber length.

Theoretical fiber orientation factor versus experimental measurements

To evaluate the influence of boundary surfaces on the fiber orientation factor, Soroushian and Lee[12] counted the number of fibers crossing the top, middle, and bottom sections of test prisms. In Fig. 5, the fiber orientation factors calculated from the proposed model are compared to the measured data as well as to the results obtained from the equation proposed by Soroushian and Lee.[12] As shown in this figure, fiber orientation factors calculated by the proposed DEM show good agreement with the measured values; the model reflects the effect of the boundary surfaces well, leading to higher values in the top and bottom regions than in the middle region of the section. Soroushian and Lee,[12] on the other hand, could not incorporate the variation of the fiber orientation factor along the cross section in their model. Moreover, the fiber orientation factor averaged over the entire region, as calculated by the proposed model, was closer to that measured.

MODEL VERIFICATION

The effects of the pullout characteristics of a fiber on the tensile stress provided by fibers, and how well these are captured by the proposed model, will be investigated in this section. The pullout characteristics of a fiber to be discussed include the slip at the frictional bond strength, s_f, the slip at the maximum tensile force provided by the mechanical anchorage of an end-hooked fiber, s_{eh}, and the ratio of the frictional bond strength to the pullout strength of an end-hooked fiber, $\tau_{f,max}/\tau_{eh,max}$.

To predict the tensile behavior of FRC members subjected to uniaxial tension, tension softening stress derived from the concrete matrix should be added to the tensile stress
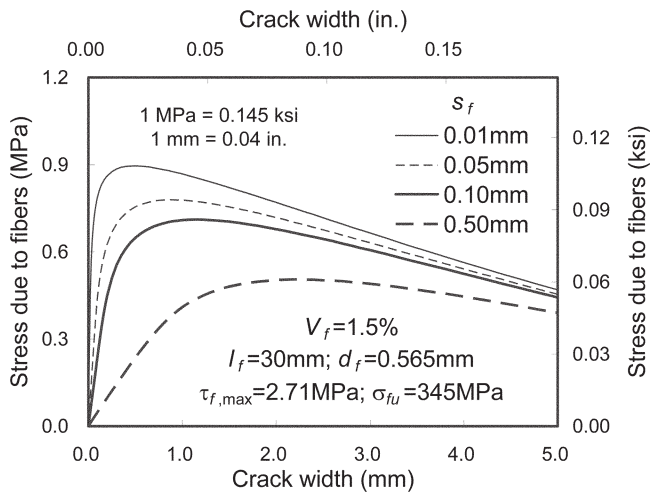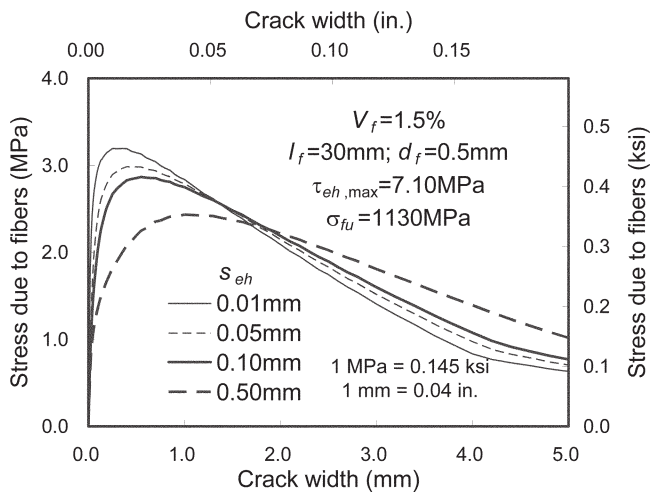
Fig. 6—Effect of s_f with straight fibers.

Fig. 7—Effect of s_eh with end-hooked fibers.

contribution derived from the fibers. For the tensile stress provided by concrete tension softening, the following model[7] has been employed.

$$f_{ct} = f_{cr}e^{-cw_{cr}} \qquad (4)$$

where c is a coefficient equal to 15 and 30 for concrete and mortar, respectively.

The pullout strength of a fiber is dependent on the fiber type and the concrete matrix. In the verification studies that follow, if the frictional bond strength or the pullout strength for a single fiber in experimental investigation was not reported in the literature, then the values given in Table 1[7] were used.

As previously discussed, fiber orientation is strongly influenced by boundary surfaces and, consequently, the effect of member dimension is a significant factor in the tensile behavior. Hence, the effect of member dimension on the tensile behavior will be discussed in this section in terms of the relationship between tensile stress and crack width. The proposed analysis model considering the effect

Table 1—Pullout strength of single fiber; taken from Voo and Foster[7]

Fiber type	Matrix	Pullout strength
Straight	Concrete	$\tau_{f,max} = 0.396\sqrt{f_c'}$ (MPa) $[4.77\sqrt{f_c'}$ (ksi)]
	Mortar	$\tau_{f,max} = 0.330\sqrt{f_c'}$ (MPa) $[3.97\sqrt{f_c'}$ (ksi)]
End-hooked	Concrete	$\tau_{eh,max} = 0.825\sqrt{f_c'}$ (MPa) $[9.94\sqrt{f_c'}$ (ksi)]
	Mortar	$\tau_{eh,max} = 0.660\sqrt{f_c'}$ (MPa) $[7.95\sqrt{f_c'}$ (ksi)]

of member dimension will be validated through comparisons with the results of experimental investigations performed by other researchers.

Effect of fiber pullout characteristics on tensile behavior of FRC

An analysis example illustrating the effect of fiber slip on the tensile stress provided by straight fibers, as a function of crack width, is shown in Fig. 6; note that s_f is the slip corresponding to the peak frictional bond strength of the fiber. The material properties of the fibers and concrete presented by Lim et. al.[11] were used in this example. Note that in this example, the effect of member dimension was not considered. As shown in this figure, the influence of fiber slip s_f on the tensile behavior of concrete members with straight fibers is significant, especially when the crack width is relatively small. With smaller values of s_f, the tensile stress provided by the fibers increases and the crack width at the peak tensile stress decreases. Although this tendency can also be predicted by the Variable Engagement Model (VEM) proposed by Voo and Foster[7] by adjusting the engagement constant as a function of the fiber diameter, the proposed model is different from VEM with respect to the evaluation procedure for the tensile stress provided by fibers. In VEM, fibers begin to contribute to the tensile behavior when a certain crack width threshold is reached, calculated by using the engagement constant and fiber inclination angle. In the proposed model, on the other hand, the tensile stress provided by fibers is calculated from the bond behavior of each fiber modeled as embedded on both sides. Thus, the proposed analysis model can be useful in the consideration of frictional bond characteristics that are dependent on the properties of the concrete matrix and fibers.

In members with end-hooked fibers, the tensile behavior of mechanical anchorage should be considered in addition to the frictional bond behavior between fibers and concrete matrix. Figure 7 shows the effect of slip at the peak tensile load by the mechanical anchorage, s_{eh}, on the tensile stress provided by fibers as a function of crack width. In this analysis example, the distance between the mechanical anchorages was 22 mm (0.87 in.), while the total fiber length was 30 mm
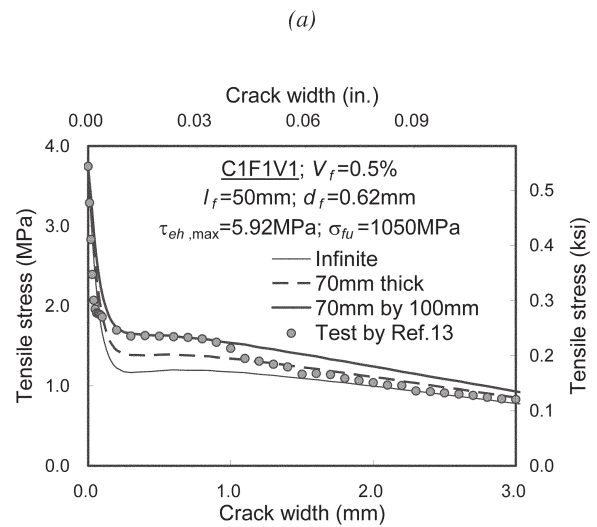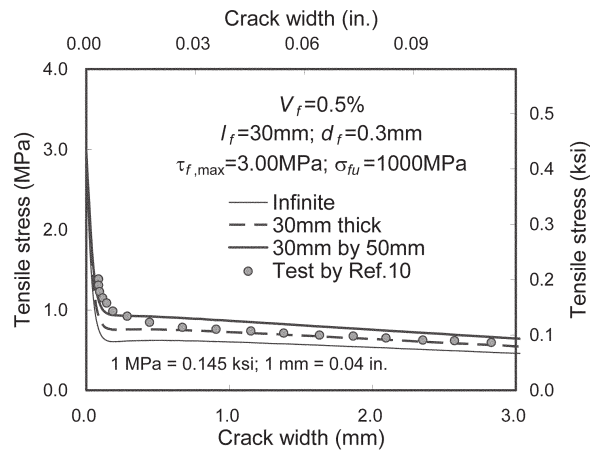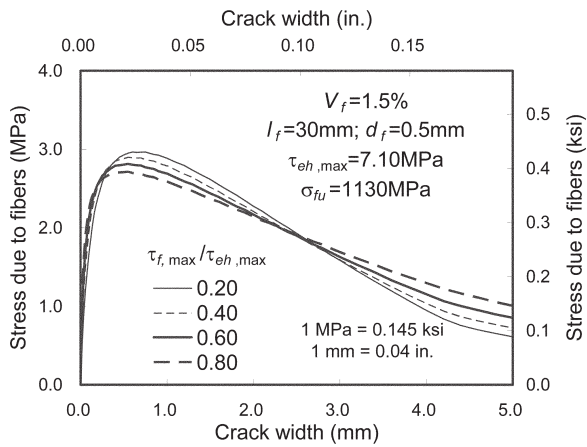
Fig. 8—Effect of $\tau_{f,max}/\tau_{eh,max}$ with end-hooked fibers.

(1.18 in.), and s_f was assumed to be 0.01 mm (0.0004 in.). For the case where only half the fiber length is embedded, using the appropriate relationship from Table 1, the bond strength due to the friction between a fiber and concrete matrix, $\tau_{f,max}$, was assumed to be 0.48 times the pullout strength, $\tau_{eh,max}$. As shown in Fig. 7, the peak tensile stress provided by end-hooked fibers increases with decreasing s_{eh}. Compared with the effect of s_f in Fig. 6, however, the tensile stress shows a much greater sensitivity to decreasing values of s_{eh}.

For FRC with end-hooked fibers, the influence of the ratio $\tau_{f,max}/\tau_{eh,max}$ ranging from 0.2 to 0.8 was investigated, as shown in Fig. 8. In this example, it was assumed that s_f = 0.01 mm (0.0004 in.) and s_{eh} = 0.1 mm (0.004 in.). It can be easily inferred that the frictional bond behavior is more dominant on the pullout strength with a longer end-hooked fiber if the same mechanical anchorage is used regardless of the fiber length. As shown in this figure, the crack width at the peak tensile stress provided by end-hooked fibers is not significantly affected by the ratio. With a smaller $\tau_{f,max}/\tau_{eh,max}$ ratio, however, the peak stress provided by end-hooked fibers increases and the postpeak behavior is steeper. As the ratio approaches 1.0, the tensile stress and crack width relationship become more similar to those of straight fibers because the frictional bond behavior becomes more dominant in the tensile behavior while the mechanical anchorage effect is diminished. Generally, the effect of the mechanical anchorage is so significant that the overall behavior of the two types of fiber turns out to be quite different. Therefore, it can be concluded that the effect of mechanical anchorage of end-hooked fibers should be considered separately from the frictional bond behavior of the fibers, as was done in the accompanying paper.[9]

Effect of member dimension on tensile behavior of FRC

Because both the average fiber stress and the fiber orientation factor are affected by member dimensions, the tensile stress provided by fibers is significantly affected by member dimensions when specimen sizes are relatively small compared to the fiber length.

To validate the proposed analysis model in its ability to consider the effects of member dimension on the tensile behavior of FRC, the specimens with straight fibers tested by Petersson[10] and the specimens with end-hooked fibers tested by Susetyo[13] were analyzed. It should be noted that the effect of the notch in the specimens tested by Petersson[10] was not

(a)

(b)

Fig. 9—Effect of member size on tensile stress due to fibers: (a) with straight fibers; and (b) with end-hooked fibers.

considered for simplicity of investigation of the member dimension effect. For the pullout characteristics of the fibers, s_f = 0.01 mm (0.0004 in.) and s_{eh} = 0.1 mm (0.004 in.) were assumed in the analyses, based on Naaman and Najm,[15] who measured slips at peak pullout load between 0.004 and 0.024 mm (0.0002 to 0.0009 in.) for smooth steel fibers, and much larger for hooked steel fibers.

Regardless of the fiber type, as shown in Fig. 9, the tensile stress capacity provided by fibers in a finite-sized member is larger than realizable in an infinite member. It can also be seen that the tensile stress measured in experiments with small specimens can be variable because it can be affected, at smaller crack widths, by the member dimensions. Moreover, the predictions made considering member dimensions showed better agreement with the test results, especially at smaller crack widths. This phenomenon is very significant in the evaluation of the serviceability of actual structures. Because the uniaxial tension specimens used to measure the tensile behavior of FRC are usually small compared to the fiber length, it can be concluded that the effect of member dimensions on the variability of test results should be taken
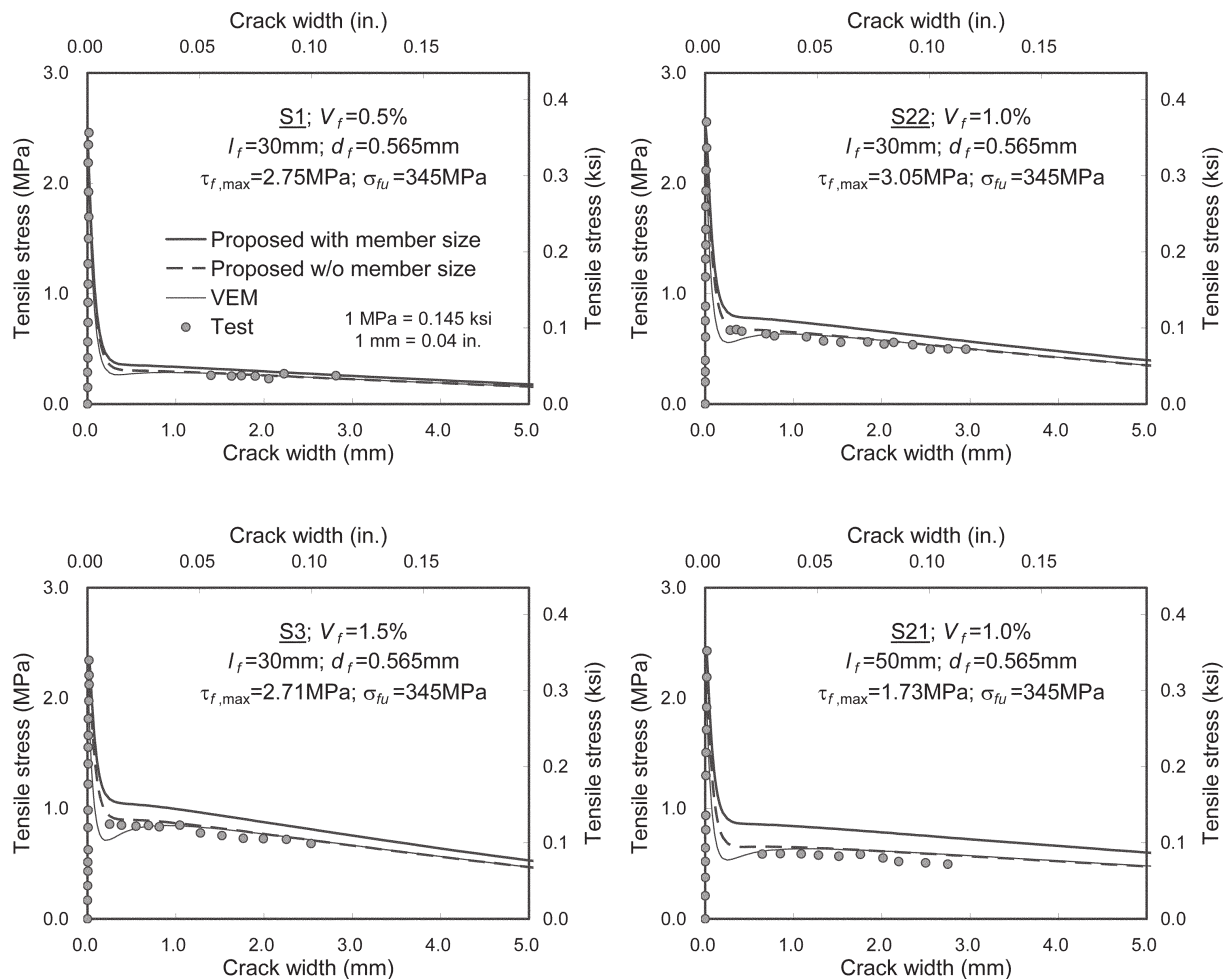
Fig. 10—Comparison with test results for members with straight fibers tested by Lim et al.[11]

into account in applications to the assessment of actual FRC structures.

Verifications of proposed model and discussions

The calculated response of 20 rectangular-section FRC members was compared with experimental data obtained from three independent investigations.[10,11,13] These studies were selected because of the availability of detailed information concerning the dimensions, properties, and tensile stress versus crack width relationship of the test specimens. The tensile stress and crack width relationship was also compared with analysis results using the VEM,[7] one of the rational recent models for FRC members considering random distribution of fibers. For the pullout characteristics of fibers, s_f = 0.01 mm (0.0004 in.) and s_{eh} = 0.1 mm (0.004 in.) were assumed in the analysis.

Straight fibers—Figure 10 shows a comparison with results from tests performed by Lim et al.[11] for members with straight fibers subjected to uniaxial tension. These specimens had a rectangular cross section of 70 mm (2.76 in.) width and 100 mm (3.94 in.) thickness. Note that size was not considered in the VEM calculations. Analysis results with the proposed DEM model are presented both with and without member dimensions considered. As shown in this figure, both the proposed analysis model without consideration of member size and VEM showed good agreement with the test results for the specimens, whereas the proposed model considering member size overestimated

the tensile stress, especially for the specimen with 50 mm (1.97 in.) straight fibers in which the fiber orientation factor was higher. Hence, it can be seen that the effect of member size can be one of the main reasons for variation or sensitivity in the tensile stress measured by small size specimens.

This potential sensitivity was investigated more clearly in Fig. 11, which examines test results by Petersson,[10] in which 30 mm (1.18 in.) straight fibers and specimens with 30 x 50 mm (1.18 x 1.97 in.) rectangular cross sections were used. In analyses performed with the proposed model, the specimen notch region was not considered when the tensile stress provided by fibers was averaged over the cross section. As seen in Fig. 11, both the analyses without considering member dimensions showed good agreement with test results for the specimens with 0.25% and 1.0% of fiber volumetric ratio, respectively, while the proposed analysis considering member dimensions showed better prediction for the specimen with 0.5% of fiber volumetric ratio. Generally, the test results fell between the results calculated with and without consideration of the member dimensions in the proposed model.

End-hooked fibers—Predictions from the proposed model were also compared to test results for end-hooked-fiber-reinforced concrete members tested by Lim et al.[11] and Susetyo.[13] It should be noted that the measured pullout strengths were used for the analysis of the specimens tested by Lim et al.,[11] while the pullout strengths presented in Table 1 were used for the specimens tested by Susetyo[13] because
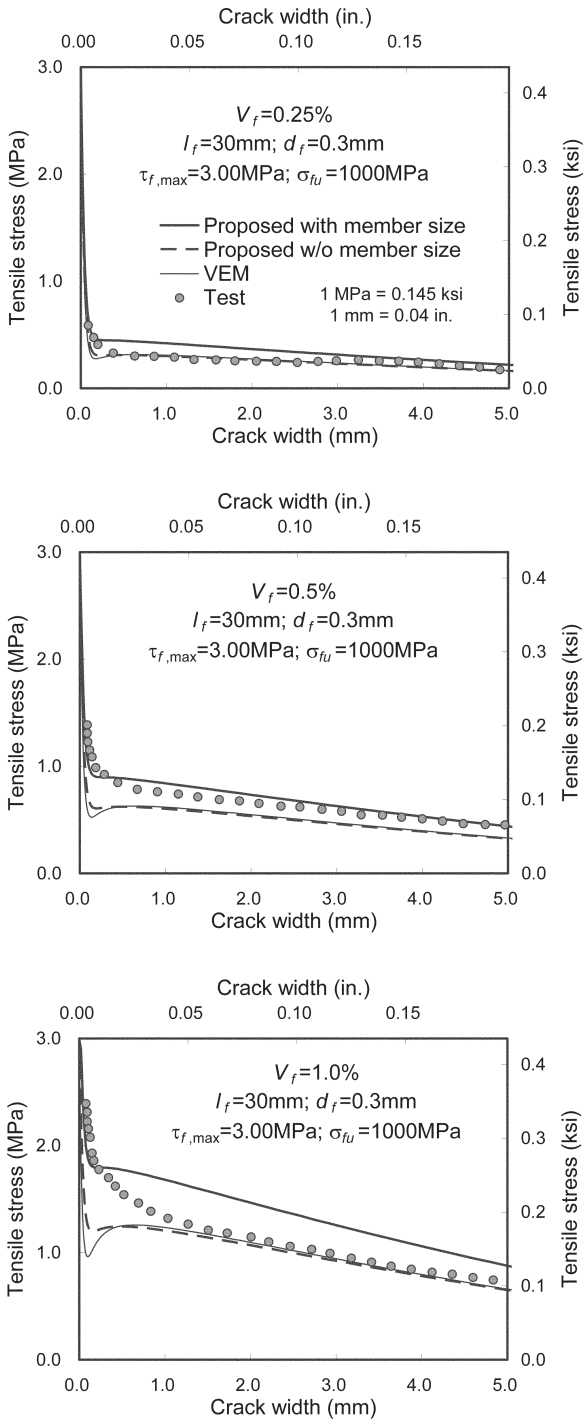
Fig. 11—Comparison with test results for members with straight fibers tested by Petersson.[10]

measured values were not reported. Based on Table 1, the ratio for $\tau_{f,max}/\tau_{eh,max}$ was assumed to 0.48.

As seen in Fig. 12 for the tests by Lim et al.,[11] while the VEM overestimated the tensile stress for crack widths larger than 1.0 mm (0.04 in.), the proposed model showed better agreement with the test results, although the tensile stress was somewhat overestimated because of the effect of member dimensions. The better correlations obtained from the DEM are much more evident in comparisons with the results obtained by Susetyo,[13] as shown in Fig. 13. While the VEM was not able to provide accurate predictions of the tensile behavior of these specimens, the experimentally

measured tensile stress versus crack width responses were generally between the analysis results predicted by the proposed model with and without the consideration of member dimension effect.

The differences in the analysis results between the proposed model and VEM are mainly due to differences in their fundamental assumptions. While VEM assumes constant bond stress along fibers—even for end-hooked fibers—the proposed model considers the frictional bond behavior and the mechanical anchorage effect separately. It can be concluded from the verification studies that the proposed model is more appropriate in the prediction of the tensile behavior of concrete members with end-hooked fibers.

Distribution of tensile stress provided by fibers

It is well known that fibers have significant beneficial effect on the tensile behavior of FRC members containing ordinary steel reinforcements, in aspects such as crack spacing, crack width, and tension stiffening.[16-22] To determine the average crack spacing, which is significant to the tension stiffening behavior, the distribution of the tensile stress provided by fibers must be accurately modeled.

The tensile stress of a fiber at the distance d_x from a crack can be calculated from the summation of the tensile stresses due to the frictional bond behavior and the mechanical anchorage as follows

$$\sigma_{f,dx} = \sigma_{f,dx,st} + \sigma_{f,dx,eh} \qquad (5)$$

where $\sigma_{f,dx,st}$ and $\sigma_{f,dx,eh}$ can be calculated considering effects from both embedded sides of a fiber using the following equations

$$\sigma_{f,dx,st} = \frac{2\tau_{short}\max(0, L_1 - d_x/\cos\theta)}{d_f} + \frac{2\tau_{long}\max(0, L_2 - d_x/\cos\theta)}{d_f} \qquad (6)$$

$$\sigma_{f,dx,eh} = \frac{2P_{eh,short}}{\pi d_f^2} + \frac{2P_{eh,long}}{\pi d_f^2} \quad \text{for } L_3 > d_x\cos\theta \qquad (7a)$$

$$\sigma_{f,dx,eh} = \frac{2P_{eh,long}}{\pi d_f^2} \quad \text{for } L_3 \le d_x\cos\theta < L_4 \qquad (7b)$$

$$\sigma_{f,dx,eh} = 0 \text{ for } L_4 \le d_x\cos\theta \qquad (7c)$$

In the above equation, $L_1 = l_a - s_{short}$, $L_1 = l_f - l_a - s_{long}$, $L_3 = l_a - s_{short} - (l_f - l_i)/2$, and $L_4 = l_f - l_a - s_{long} - (l_f - l_i)/2$.

Considering the random distribution of fibers, the tensile stress provided by fibers at the distance d_x from a crack can be calculated for 3-D infinite elements from Eq. (1) to (2) and Eq. (5) to (7), as follows

$$f_{f,dx} = 0.5V_f \cdot \frac{l_f}{2}\int_0^{l_f/2}\int_0^{\pi/2}\sigma_{f,dx}(l_a,\theta)\sin\theta d\theta dl_a \qquad (8)$$

Figure 14 shows the attenuation of the fiber tensile stress with distance from the crack for several crack widths. The material properties for the fibers and concrete matrix used in this analysis example were presented by Bischoff,[18] who investigated the effect of end-hooked steel fibers on the tension
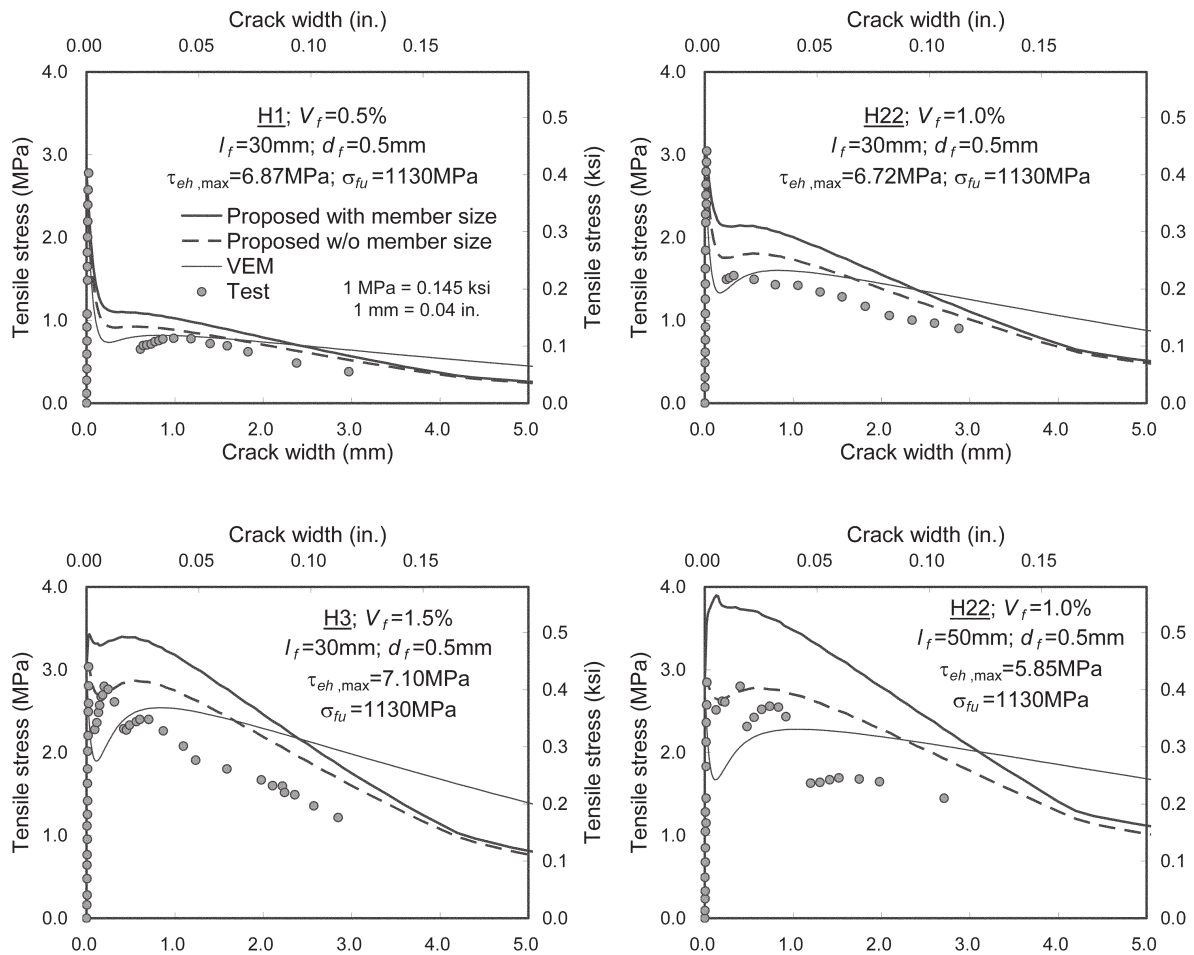
Fig. 12—Comparison with test results for members with end-hooked fibers tested by Lim et al.[11]

stiffening and the cracking behavior of FRC with ordinary steel reinforcements. For the analysis example with the straight fibers, only the pullout strength of the fiber was changed from that of the end-hooked fibers according to Table 1. As shown in Fig. 14, the tensile stress provided by fibers is almost completely transferred to the concrete matrix within a distance of 0.7 times the fiber length from a crack for straight fibers or 0.8 times for the end-hooked fibers, respectively, because the probability for fibers with a small fiber inclination angle is small. In addition, it can be seen that the slope for the distribution of the tensile stress by fibers in the member with the straight fibers is little affected by the crack width, whereas the slope with the end-hooked fibers is significantly affected at crack widths larger than 0.3 mm (0.012 in.) because some of fibers ruptured given the high pullout strength and the low fiber tensile strength. These analysis results indicate that the simple linear assumption[21] for the distribution of tensile stress provided by fibers is not appropriate for use in predictions of the average crack spacing which, in turn, has a significant influence on the evaluation of tension stiffening in FRC members containing ordinary steel reinforcement. The distribution of the fiber tensile stress calculated from Eq. (5) to (8), thus, can be useful for the analysis of FRC members with conventional reinforcement subjected to tension.

CONCLUSIONS
Behaviors predicted by the proposed Diverse Embedment Model (DEM) for FRC in tension were compared with experimental results in regards to the fiber orientation factor and the tensile stress versus crack width relationship. Findings and conclusions are summarized as follows:

1. Expanded from previous researchers' results,[7,8,14] the fiber orientation factor has been mathematically evaluated with the proposed analysis model considering the influence of boundary surfaces. It shows that the fiber orientation factor varies within a member cross section because the fiber orientation is significantly influenced by boundary surfaces. The calculated fiber orientation factors were higher near boundary surfaces, consistent with measured data. It can be concluded that when a member dimension is less than two times the fiber length, the effect of the member dimension should be considered in determining an averaged fiber orientation factor for the cross section. The fiber orientation factor, in turn, will directly affect the tensile stress response provided by the fibers.

2. The proposed analysis model predicted well the test results not only for straight fibers but also for end-hooked fibers. The Variable Engagement Model (VEM)[7] predicted well only the results for straight fibers. The improved capability is primarily due to differences in the fundamental assumptions of each model; the proposed model considers both the frictional bond behavior and the mechanical anchorage effect separately, whereas the VEM assumes constant bond stress along fibers, even for end-hooked fibers. Thus, the proposed model is more appropriate for the prediction of the tensile behavior of concrete members with end-hooked fibers.

3. The distribution of the tensile stresses sustained by fibers can be calculated by the proposed model. These distributions can then be used in an analysis of the tensile behavior of FRC members containing ordinary steel reinforcement, to better simulate various aspects of response, including average crack spacing and tension stiffening effect.
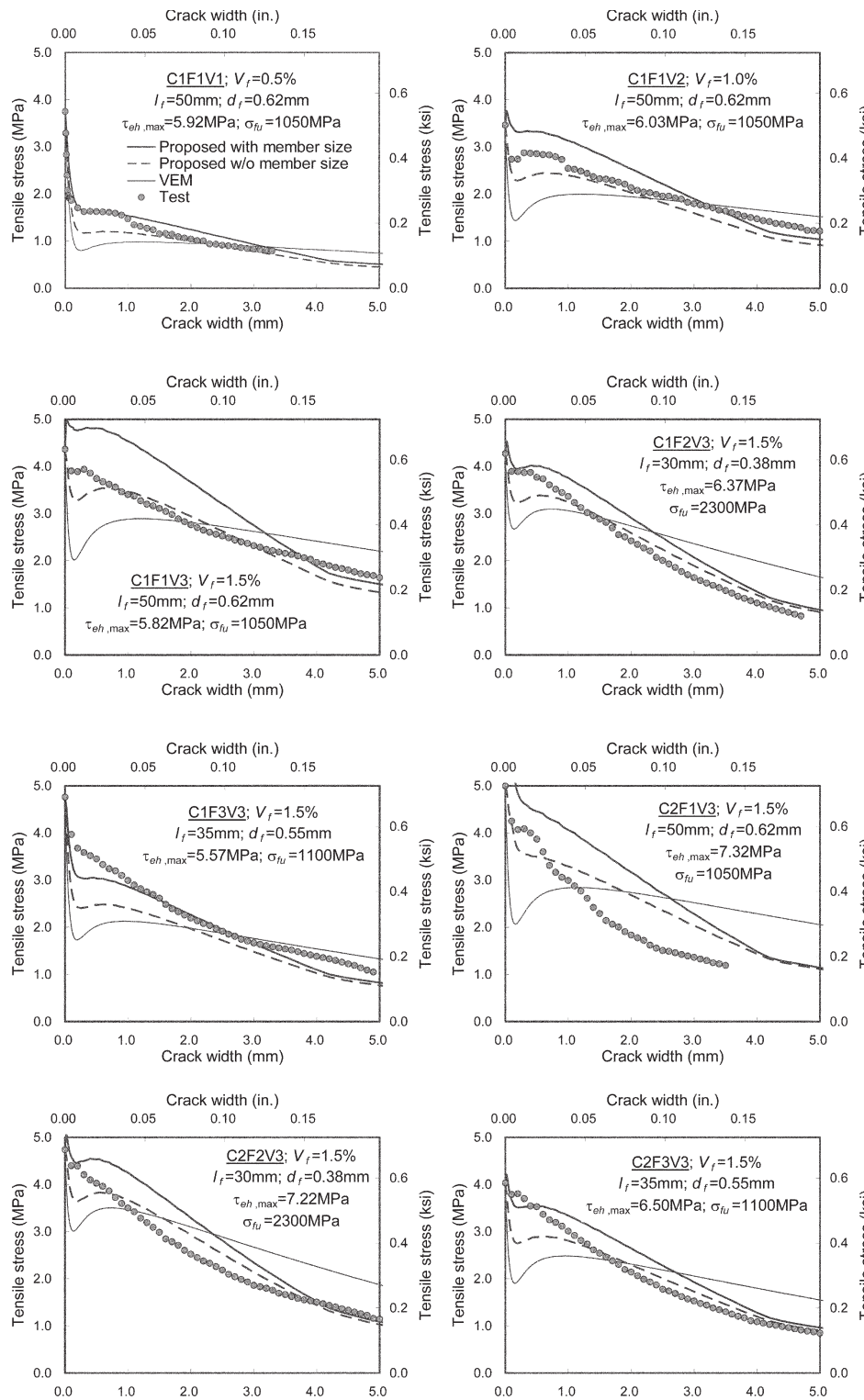
Fig. 13—Comparison of test results for members with end-hooked fibers test by Susetyo.[13]

NOTATION

|		
b	=	member width
c	=	coefficient for concrete/mortar tension softening
d_c	=	distance from boundary surface in 2-D element
d_{cy}, d_{cz}	=	distances from boundary surface to Y and Z axis in 3-D element, respectively
d_f	=	fiber diameter
d_x	=	distance from crack
f_c'	=	concrete compressive strength
f_{cr}	=	cracking strength of concrete or mortar
f_{ct}	=	tensile stress by the concrete/mortar tension softening at a given crack width
f_f	=	tensile stress provided by fibers at a given crack width
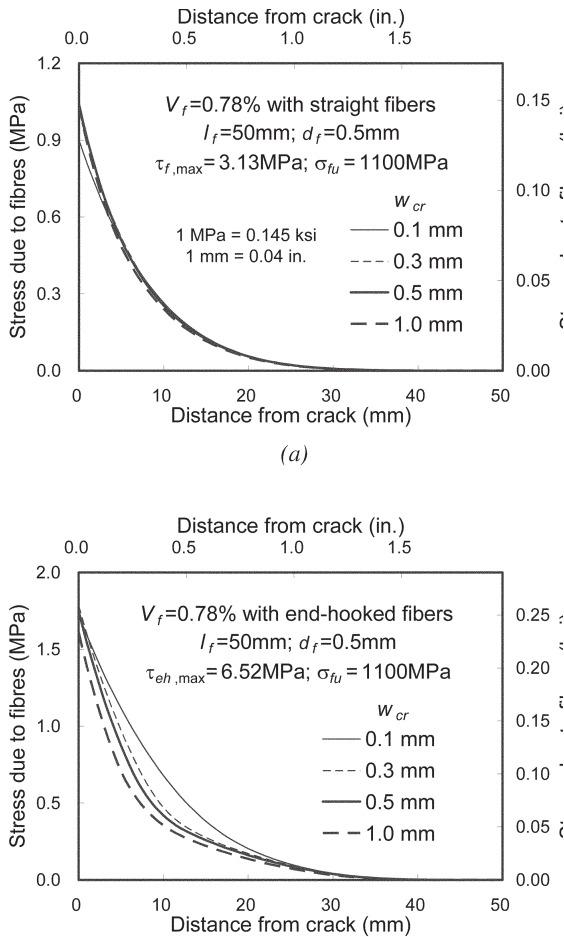
Fig. 14—Attenuation of fiber tensile stress with distance from crack: (a) straight fibers; and (b) end-hooked fibers.

$f_{f,dx}$	=	tensile stress by fibers at distance d_x from a crack
h	=	member thickness
l_a	=	fiber embedment length for the shorter embedded part across a crack
l_f	=	fiber length
l_i	=	distance between mechanical anchorages for an end-hooked fiber
$P_{eh,long}$,		
$P_{eh,short}$	=	tensile forces by mechanical anchorage of the longer and shorter embedded part of an end-hooked fiber, respectively
$P_{eh,max}$	=	maximum tensile force due to the mechanical anchorage of an end-hooked fiber
s_{eh}	=	slip at $P_{eh,max}$
s_f	=	slip at the frictional bond strength for fiber with inclination angle of 0 degrees
s_{long}	=	slip at crack for longer embedded part of fiber
s_{short}	=	slip at crack for shorter embedded part of fiber
V_f	=	fiber volumetric ratio
w_{cr}	=	crack width
α_f	=	fiber orientation factor
$\alpha_{f,avg}$	=	fiber orientation factor averaged through member thickness or cross section
θ	=	fiber inclination angle from axis perpendicular to crack surface
$\sigma_{f,cr}$	=	fiber stress at a crack with a given fiber inclination angle and embedment length
$\sigma_{f,cr,avg}$	=	average fiber stress at a crack considering random distributions of fiber inclination angle and embedment length
$\sigma_{f,cr,exp}$	=	maximum experienced fiber stress at crack
$\sigma_{f,dx}$	=	tensile stress of a fiber at distance d_x from a crack considering frictional bond behavior as well as mechanical anchorage
$\sigma_{f,dx,st}$,		
$\sigma_{f,dx,eh}$	=	tensile stresses of a fiber at distance d_x from a crack by frictional bond behavior and mechanical anchorage, respectively
σ_{fu}	=	ultimate tensile strength of fiber
$\tau_{eh,max}$	=	pullout strength of end-hooked fiber
$\tau_{f,max}$	=	frictional pullout strength for end-hooked fiber or straight fiber
τ_{long}, τ_{short}	=	frictional bond stress for longer and shorter embedded part of fiber, respectively

REFERENCES

1. Nammur, G., and Naaman, A. E., "Bond Stress Model for Fiber Reinforced Concrete Based on Bond Stress-Slip Relationship," *ACI Materials Journal*, V. 86, No. 1, Jan.-Feb. 1989, pp. 45-57.

2. Naaman, A. E.; Nammur, G. G.; Alwan, J. M.; and Najm, H. S., "Fiber Pullout and Bond Slip. I: Analytical Study," *Journal of Structural Engineering*, ASCE, V. 117, No. 9, Sept. 1991, pp. 2769-2790.

3. Naaman, A. E.; Namur, G. G.; Alwan, J. M.; and Najm, H. S., "Fiber Pullout and Bond Slip. II: Experimental Validation," *Journal of Structural Engineering*, ASCE, V. 117, No. 9, Sept. 1991, pp. 2791-2800.

4. Sujivorakul, C.; Waas, A. M.; and Naaman, A. E., "Pullout Response of a Smooth Fiber with an End Anchorage," *Journal of Engineering Mechanics*, ASCE, V. 126, No. 9, Sept. 2000, pp. 986-993.

5. Marti, P.; Pfyl, T.; Sigrist, V.; and Ulaga, T., "Harmonized Test Procedures for Steel Fiber-Reinforced Concrete," *ACI Materials Journal*, V. 96, No. 6, Nov.-Dec. 1999, pp. 676-686.

6. Foster, S. J., "On Behavior of High-Strength Concrete Columns: Cover Spalling, Steel Fibers, and Ductility," *ACI Structural Journal*, V. 98, No. 4, July-Aug. 2001, pp. 583-589.

7. Voo, J. Y. L., and Foster, S. J., "Variable Engagement Model for Fibre Reinforced Concrete in Tension," *Uniciv Report* No. R-420, School of Civil and Environmental Engineering, University of New South Wales, June 2003, 86 pp.

8. Stroeven, P., "Stereological Principles of Spatial Modeling Applied to Steel Fiber-Reinforced Concrete in Tension," *ACI Materials Journal*, V. 106, No. 3, May-June 2009, pp. 213-222.

9. Lee, S.-C.; Cho, J.-Y.; and Vecchio, F. J., "Diverse Embedment Model for Steel Fiber-Reinforced Concrete in Tension: Model Development," *ACI Materials Journal*, V. 108, No. 5, Sept.-Oct 2011, pp. 516-525.

10. Petersson, P. E., "Fracture Mechanical Calculations and Tests for Fiber-Reinforced Cementitious Materials," *Proceedings of Advances in Cement-Matrix Composites*, Materials Research Society, Boston, 1980, pp. 95-106.

11. Lim, T. Y.; Paramasivam, P.; and Lee, S. L., "Analytical Model for Tensile Behavior of Steel-Fiber Concrete," *ACI Materials Journal*, V. 84, No. 4, July-Aug. 1987, pp. 286-298.

12. Soroushian, P., and Lee, C.-D., "Distribution and Orientation of Fibers in Steel Fiber Reinforced Concrete," *ACI Materials Journal*, V. 87, No. 5, Sept.-Oct. 1990, pp. 433-439.

13. Susetyo, J., "Fibre Reinforcement for Shrinkage Crack Control in Prestressed, Precast Segmental Bridges," Doctorate thesis, University of Toronto, Toronto, ON, Canada, 2009, 307 pp.

14. Aveston, J., and Kelly, A., "Theory of Multiple Fracture of Fibrous Composites," *Journal of Materials Science*, V. 8, 1973, pp. 352-362.

15. Naaman, A. E., and Najm, H., "Bond-Slip Mechanisms of Steel Fibers in Concrete," *ACI Materials Journal*, V. 88, No. 2, Mar.-Apr. 1991, pp. 135-145.

16. Abrishami, H. H., and Mitchell, D., "Influence of Steel Fibers on Tension Stiffening," *ACI Structural Journal*, V. 94, No. 6, Nov.-Dec. 1997, pp. 769-776.

17. Noghabai, K., "Behavior of Tie Elements of Plain and Fibrous Concrete and Varying Cross Sections," *ACI Structural Journal*, V. 97, No. 2, Mar.-Apr. 2000, pp. 277-285.

18. Bischoff, P. H., "Tension Stiffening and Cracking of Steel Fiber-Reinforced Concrete," *Journal of Materials in Civil Engineering*, ASCE, V. 15, No. 2, Apr. 2003, pp. 174-182.

19. Fantilli, A. P., and Vallini, P., "Tension Stiffening Range in FRC Elements," Sixth RILEM Symposium on Fibre Reinforced Concrete-BEFIB 2004, RILEM Proceedings PRO39, RILEM Publication, Bagneux, France, Sept. 2004, pp. 847-856.

20. Fantilli, A. P.; Mihashi, H.; and Vallini, P., "Strain Compatibility between HPFRCC and Steel Reinforcement," *Materials and Structures*, V. 38, May 2005, pp. 495-503.

21. Leutbecher, T.; and Fehling E., "Crack Width Control for Combined Reinforcement of Rebars and Fibers Exemplified by Ultra-High-Performance Concrete," *fib* Task Group 8.6, Ultra High Performance Fiber Reinforced Concrete – UHPFRC, Sept. 2008, pp. 1-28.

22. Hameed, R.; Turatsinze, A.; Duprat, F.; and Sellier, A., "A Study on Reinforced Fibrous Concrete Elements Subjected to Uniaxial Tensile Loading," *KSCE Journal of Civil Engineering*, V. 14, No. 4, 2010, pp. 547-556.